HIGH-FIDELITY UNIVERSAL QUANTUM GATES THROUGH GROUP-SYMMETRIZED RAPID PASSAGE

RAN LI

Department of Physics, Kent State University, Stark Campus
North Canton, OH 44720;
Advanced Sciences Institute, The Institute of Physical and Chemical Research (RIKEN)
Wako-shi, Saitama 351-0198, Japan;
CREST, Japan Science and Technology Agency (JST)
Kawaguchi, Saitama 332-0012, Japan

FRANK GAITAN[ab]

Advanced Sciences Institute, The Institute of Physical and Chemical Research (RIKEN)
Wako-shi, Saitama 351-0198, Japan;
CREST, Japan Science and Technology Agency (JST)
Kawaguchi, Saitama 332-0012, Japan

Twisted rapid passage is a type of non-adiabatic rapid passage that generates controllable quantum interference effects that were first observed experimentally in 2003. It is shown that twisted rapid passage sweeps can be used to implement a universal set of quantum gates $\mathcal{G}_U$ that operate with high-fidelity. The gate set $\mathcal{G}_U$ consists of the Hadamard and NOT gates, together with variants of the phase, $\pi/8$, and controlled-phase gates. For each gate g in $\mathcal{G}_U$, sweep parameter values are provided which simulations indicate will produce a unitary operation that approximates g with error probability$P_e < 10^{-4}$. Note that *all* gates in $\mathcal{G}_U$ are implemented using a *single family* of control-field, and the error probability for each gate falls below the rough-and-ready estimate for the accuracy threshold $P_a \sim 10^{-4}$.

Keywords: fault-tolerant quantum computing, accuracy threshold, quantum interference, group-symmetrized evolution, non-adiabatic dynamics

1 Introduction

The accuracy threshold theorem [1–8] provides the impetus for the work presented in this paper. This remarkable theorem established that an arbitrary quantum computation could be done with an arbitrarily small error probability, in the presence of noise, and using imperfect quantum gates, if the following conditions are satisfied. (1) The computational data is protected by a sufficiently layered concatenated quantum error correcting code. (2) Fault-

[a]Corresponding author: fgaitan@lps.umd.edu
[b]Permanent Address: Laboratory for Physical Sciences, 8050 Greenmead Drive, College Park, MD 20740.

tolerant protocols for quantum computation, error correction, and measurement are used. (3) A universal set of *unencoded* quantum gates is available with the property that each gate in the set has an error probability P_e that falls below a value P_a known as the accuracy threshold. The value of the threshold is model-dependent, though for many, $P_a \sim 10^{-4}$ has become a rough-and-ready estimate. Thus gates are anticipated to be approaching the accuracies needed for fault-tolerant quantum computing when $P_e < 10^{-4}$. One of the principal challenges facing the field of quantum computing is determining how to implement a universal set of unencoded quantum gates for which all gate error probabilities satisfy $P_e < 10^{-4}$.

In this paper numerical simulation results are presented which indicate that a class of non-adiabatic rapid passage sweeps, first realized experimentally in 1991 [9], and known as twisted rapid passage (TRP), should be capable of implementing a universal set of unencoded quantum gates $\mathcal{G}_U$ that operate non-adiabatically and with gate error probabilities satisfying $P_e < 10^{-4}$. The gate set $\mathcal{G}_U$ consists of the one-qubit Hadamard and NOT gates, together with variants of the one-qubit $\pi/8$ and phase gates, and the two-qubit controlled-phase gate. The universality of $\mathcal{G}_U$ was demonstrated in Ref. [10]. This level of gate accuracy is largely due to controllable quantum interference effects that arise during a TRP sweep [11, 12], and which were observed in 2003 using NMR [13]. To find TRP sweep parameter values that yield such high-performance quantum gates, it proved necessary to combine numerical simulation of the Schrodinger dynamics with optimization algorithms that search for minima of P_e. In the case of the two-qubit modified controlled-phase gate, to achieve $P_e < 10^{-4}$, it was also necessary to interleave the TRP sweep with the group-symmetrized evolution of Ref. [14].

The outline of this paper is as follows. Following this Introduction, Section 2 summarizes the essential properties of TRP, and how the numerical simulation and optimization are done. In Section 3 we explain how group-symmetrized evolution is incorporated into a TRP sweep, and then present our simulation results for each of the gates in $\mathcal{G}_U$ in Section 4. We close in Section 5 with a summary of our results, and a discussion of possible directions for future work.

2 Twisted Rapid Passage

This Section presents the essential properties of twisted rapid passage (TRP). A more detailed presentation of the discussion in Sections 2.1 and 2.2 appears in Refs. [10] and [12]. In an effort to make the present paper more self-contained, we summarize that discussion here. Section 2.1 introduces TRP as a generalization of adiabatic rapid passage in which the control-field twists in the x-y plane at the same time that its z-component undergoes a non-adiabatic inversion. We describe how controllable quantum interference effects arise as a consequence of the twisting. Section 2.2 discusses the details of the numerical simulations, and describes the optimization procedures used to find minima of the gate error probability.[a]

2.1 TRP Essentials

To introduce TRP [11, 12], we consider a single-qubit interacting with an external control-field $\mathbf{F}(t)$ via the Zeeman interaction $H_z(t) = -\boldsymbol{\sigma} \cdot \mathbf{F}(t)$, where σ_i are the Pauli matrices ($i = x, y, z$). TRP is a generalization of adiabatic rapid passage (ARP) [15]. In ARP, the control-field $\mathbf{F}(t)$ is slowly inverted over a time T_0 such that $\mathbf{F}(t) = at\,\hat{\mathbf{z}} + b\,\hat{\mathbf{x}}$. In TRP,

[a]As will be seen shortly, we actually search for minima of an upper bound of the gate error probability.

however, the control-field is allowed to twist in the x-y plane with time-varying azimuthal angle $\phi(t)$, while simultaneously undergoing inversion along the z-axis:

$$\mathbf{F}(t) = at\,\hat{\mathbf{z}} + b\,\cos\phi(t)\,\hat{\mathbf{x}} + b\,\sin\phi(t)\,\hat{\mathbf{y}}. \tag{1}$$

Here $-T_0/2 \leq t \leq T_0/2$, and throughout this paper, we consider TRP with *non-adiabatic* inversion. As shown in Ref. [12], the qubit undergoes resonance when

$$at - \frac{\hbar}{2}\frac{d\phi}{dt} = 0. \tag{2}$$

For polynomial twist, the phase profile $\phi(t)$ takes the form

$$\phi_n(t) = \frac{2}{n}Bt^n. \tag{3}$$

In this case, Eq. (2) has $n-1$ roots, though only real-valued roots correspond to resonance. Ref. [11] showed that for $n \geq 3$, the qubit undergoes resonance multiple times during a *single* TRP sweep: (i) for all $n \geq 3$, when $B > 0$; and (ii) for odd $n \geq 3$, when $B < 0$. For the remainder of this paper we restrict ourselves to $B > 0$, and to *quartic* twist for which $n = 4$ in Eq. (3). During quartic twist, the qubit passes through resonance at times $t = 0, \pm\sqrt{a/\hbar B}$ [11]. It is thus possible to vary the time separating the resonances by varying the TRP sweep parameters B and a.

Ref. [11] showed that these multiple resonances have a strong influence on the qubit transition probability, allowing transitions to be strongly enhanced or suppressed through a small variation of the sweep parameters. Ref. [16] calculated the qubit transition amplitude to all orders in the non-adiabatic coupling. The result found there can be re-expressed as the following diagrammatic series:

$T_{-}(t) =$ 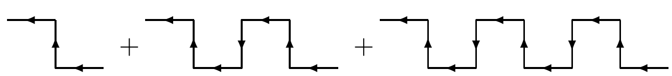 $+ \quad \cdots \quad .$ (4)

Lower (upper) lines correspond to propagation in the negative (positive) energy-level, and the vertical lines correspond to transitions between the two energy-levels. The calculation sums the probability amplitudes for all interfering alternatives [17] that allow the qubit to end up in the positive energy-level given that it was initially in the negative energy-level. As we have seen, varying the TRP sweep parameters varies the time separating the resonances. This in turn changes the value of each diagram in Eq. (4), and thus alters the interference between the alternative transition pathways. It is the sensitivity of the individual alternatives/diagrams to the time separation of the resonances that allows TRP to manipulate this quantum interference. Zwanziger et al. [13] observed these interference effects in the transition probability using NMR and found quantitative agreement between theory and experiment. It is this link between interfering quantum alternatives and the TRP sweep parameters that we believe underlies the ability of TRP to drive high-fidelity (non-adiabatic) one- and two-qubit gates.

2.2 Simulation and Optimization Procedures

As is well-known, the Schrodinger dynamics is driven by a Hamiltonian $H(t)$ which causes a unitary transformation U to be applied to an initial quantum state $|\psi\rangle$. In this paper, it

is assumed that the Hamiltonian $H(t)$ contains terms that Zeeman-couple each qubit to the TRP control-field $\mathbf{F}(t)$. Assigning values to the TRP sweep parameters (a, b, B, T_0) fixes the control-field $\mathbf{F}(t)$, and in turn, the actual unitary transformation U_a applied to $|\psi\rangle$. The task is to find TRP sweep parameter values that produce an applied gate U_a that approximates a desired target gate U_t sufficiently closely that its error probability (defined below) satisfies $P_e < 10^{-4}$. In the following, the target gate U_t will be one of the gates in the universal set $\mathcal{G}_U$. Since $\mathcal{G}_U$ contains only one- and two-qubit gates, our simulations will only involve one- and two-qubit systems.

For the *one-qubit simulations*, the Hamiltonian $H_1(t)$ is the Zeeman Hamiltonian $H_z(t)$ introduced in Section 2.1. Ref. [12] showed that it can be written in the following dimensionless form:

$$\mathcal{H}_1(\tau) = (1/\lambda)\left\{-\tau\sigma_z - \cos\phi_4(\tau)\sigma_x - \sin\phi_4(\tau)\sigma_y\right\}. \tag{5}$$

Here: $\tau = (a/b)t$; $\lambda = \hbar a/b^2$; and for quartic twist, $\phi_4(\tau) = (\eta_4/2\lambda)\tau^4$, with $\eta_4 = \hbar B b^2/a^3$.

For the *two-qubit simulations*, the Hamiltonian $H_2(t)$ contains terms that Zeeman-couple each qubit to the TRP control-field, and an Ising interaction term that couples the two qubits. Alternative two-qubit interactions can easily be considered, though all simulation results presented below assume an Ising interaction between the qubits. To break a resonance-frequency degeneracy $\omega_{12} = \omega_{34}$ for transitions between, respectively, the ground and first-excited states ($E_1 \leftrightarrow E_2$) and the second- and third excited states ($E_3 \leftrightarrow E_4$), the term $c_4|E_4(t)\rangle\langle E_4(t)|$ was added to $H_2(t)$. Combining all of these remarks, we arrive at the following (dimensionless) two-qubit Hamiltonian [10]:

$$\begin{aligned}\mathcal{H}_2(\tau) \;=\; & \left[-(d_1+d_2)/2 + \tau/\lambda\right]\sigma_z^1 - (d_3/\lambda)\left[\cos\phi_4\sigma_x^1 + \sin\phi_4\sigma_y^1\right] \\ & + \left[-d_2/2 + \tau/\lambda\right]\sigma_z^2 \;\; - (1/\lambda)\left[\cos\phi_4\sigma_x^2 + \sin\phi_4\sigma_y^2\right] \\ & -(\pi d_4/2)\sigma_z^1\sigma_z^2 \;\; + c_4|E_4(\tau)\rangle\langle E_4(\tau)|.\end{aligned} \tag{6}$$

Here: (i) $b_i = \hbar\gamma_i B_{rf}/2$, $\omega_i = \gamma_i B_0$, γ_i is the gyromagnetic ratio for qubit i, and $i = 1, 2$; (ii) $\tau = (a/b_2)t$, $\lambda = \hbar a/b_2^2$, and $\eta_4 = \hbar B b_2^2/a^3$; and (iii) $d_1 = (\omega_1 - \omega_2)b_2/a$, $d_2 = (\Delta/a)b_2$, $d_3 = b_1/b_2$, and $d_4 = (J/a)b_2$, where Δ is a detuning parameter [10].

The numerical simulations assign values to the TRP sweep parameters and then integrate the Schrodinger equation to obtain the unitary transformation U_a produced by the resulting TRP sweep. Given U_a, U_t, and the initial state $|\psi\rangle$, it is possible to work out [12] the error probability $P_e(\psi)$ for the TRP final state $|\psi_a\rangle = U_a|\psi\rangle$, relative to the target final state $|\psi_t\rangle = U_t|\psi\rangle$. The gate error probability P_e is defined to be the worst-case value of $P_e(\psi)$:

$$P_e \equiv \max_{|\psi\rangle} P_e(\psi). \tag{7}$$

It proves useful at this point to introduce the positive operator

$$P = \left(U_a^\dagger - U_t^\dagger\right)\left(U_a - U_t\right). \tag{8}$$

Ref. [12] showed that the error probability P_e satisfies the upper bound

$$P_e \leq Tr\, P, \tag{9}$$

where the RHS is the trace of the positive operator P. Once U_a is known, $Tr\,P$ is easily evaluated, and so it is a convenient proxy for P_e which is harder to calculate. $Tr\,P$ also has the virtue of being directly related to the gate fidelity

$$\mathcal{F}_n = \left(\frac{1}{2^n}\right) Re\left[\,Tr\left(U_a^\dagger U_t\right)\,\right], \tag{10}$$

where n is the number of qubits acted on by the gate. It is straightforward to show [10] that

$$\mathcal{F}_n = 1 - \left(\frac{1}{2^{n+1}}\right) Tr\,P. \tag{11}$$

The simulations calculate $Tr\,P$, which is then used to upper bound the gate error probability P_e via Eq. (9).

To find TRP sweep parameter values that yield highly accurate non-adiabatic quantum gates, it proved necessary to combine the numerical simulations with function minimization algorithms [18] that search for sweep parameter values that minimize the $Tr\,P$ upper bound. The multi-dimensional downhill simplex method was used for the one-qubit gates, while simulated annealing was used for the two-qubit modified controlled-phase gate. This produced the one-qubit gate results that will be presented in Section 4.1. However, for the modified controlled-phase gate, simulated annealing was only able to find sweep parameter values that gave $P_e \leq 1.27 \times 10^{-3}$ [10]. To further improve the performance of this two-qubit gate, it proved necessary to incorporate the group-symmetrized evolution of Ref. [14] to obtain a modified controlled-phase gate with $P_e < 10^{-4}$. In the following Section we describe how group-symmetrized evolution is incorporated into a TRP sweep.

3 Group-symmetrized Evolution and TRP

Ref. [14] introduced a unitary group-symmetrization procedure that yields an effective dynamics that is invariant under the action of a finite group $\mathcal{G}$. To incorporate this group-symmetrization into a TRP sweep, the first step is to identify the group $\mathcal{G}$ with a finite symmetry group of the target gate U_t, and then apply the procedure of Ref. [14] to filter out the $\mathcal{G}$-noninvariant part of the TRP dynamics. As the $\mathcal{G}$-noninvariant dynamics is manifestly bad dynamics relative to U_t, group-symmetrized TRP yields a better approximation to U_t. In this section we describe how group-symmetrization works, and then show how it can be incorporated into a TRP sweep. The simulation results presented in Section 4.2 for the two-qubit modified controlled-phase gate are for a group-symmetrized TRP sweep.

3.1 Static Hamiltonian

Consider a quantum system $\mathcal{Q}$ with time-independent Hamiltonian H and Hilbert space $\mathcal{H}$. The problem is to provide $\mathcal{Q}$ with an effective dynamics that is invariant under a finite group $\mathcal{G}$, even when H itself is *not* $\mathcal{G}$-invariant. This symmetrized dynamics manifests as a $\mathcal{G}$-invariant effective propagator $\tilde{U}$ that evolves the system state over a time t. Let $\{\rho_i = \rho(g_i)\}$ be a unitary representation of $\mathcal{G}$ on $\mathcal{H}$, and let $|\mathcal{G}|$ denote the order of $\mathcal{G}$. The procedure begins by partitioning the time-interval $(0,t)$ into N subintervals of duration $\Delta t_N = t/N$, and then further partioning each subinterval into $|\mathcal{G}|$ smaller intervals of duration $\delta t_N = \Delta t_N/|\mathcal{G}|$. Let $\delta U_N = \exp\left[-(i/\hbar)\delta t_N H\right]$ denote the H-generated propagator for a time-interval δt_N,

and assume that the time to apply each $\rho_i \in \mathcal{G}$ is negligible compared to δt_N (bang-bang limit [19]). In each subinterval, the following sequence of transformations is applied:

$$U(\Delta t_N) = \prod_{i=1}^{|\mathcal{G}|} \rho_i^\dagger \delta U_N \rho_i. \tag{12}$$

The propagator $\tilde{U}$ over the full time-interval $(0, t)$ is then

$$\tilde{U} = \lim_{N\to\infty} \left[U(\Delta t_N)\right]^N. \tag{13}$$

Ref. [14] showed that:

1. for $N \gg 1$, $U(\Delta t_N) \to \exp\left[-(i/\hbar)\Delta t_N \tilde{H}\right]$, where $\tilde{H} = (1/|\mathcal{G}|)\sum_{i=1}^{|\mathcal{G}|} \rho_i^\dagger H \rho_i$;
2. $\tilde{H}$ is $\mathcal{G}$-invariant (viz. $[\tilde{H}, \rho_i] = 0$ for all $\rho_i \in \mathcal{G}$);
3. the propagator $\tilde{U}$ over $(0, t)$ is $\tilde{U} = \exp\left[-(i/\hbar)t\tilde{H}\right]$, which is $\mathcal{G}$-invariant due to the $\mathcal{G}$-invariance of $\tilde{H}$.

The outcome of this procedure is an effective propagator $\tilde{U}$ that is $\mathcal{G}$-invariant as desired.

3.2 Time-varying Hamiltonian

In this subsection we show how the above procedure can be generalized to allow for a time-varying Hamiltonian $H(t)$ which is the appropriate context for a TRP sweep. Although the generalization is straight-forward, we are not aware of any prior treatment of group-symmetrized evolution in the presence of a time-dependent Hamiltonian. The essential idea is to divide the time interval $(0, t)$ into sufficiently small subintervals that $H(t)$ is effectively constant in each. The above time-independent argument can be then be applied to each subinterval, yielding a $\mathcal{G}$-symmetrized propagator for that subinterval. Time-ordering the subinterval effective propagators then gives the effective group-symmetrized propagator for the entire interval $(0, t)$. Having sketched out the basic idea, we now present the details.

Consider a quantum system $\mathcal{Q}$ evolving under the action of a time-varying Hamiltonian $H(t)$. We begin again by partitioning the time-interval $(0, t)$ into $\mathcal{N}$ subintervals (t_{i-1}, t_i) of duration $\Delta t_{\mathcal{N}} = t/\mathcal{N}$, where $i = 1, \ldots, \mathcal{N}$. The number of subintervals is chosen sufficiently large that $H(t)$ is effectively constant over each subinterval: $H(t) \approx H(t_i)$ for all $t \in (t_{i-1}, t_i)$. We estimate the value of $\mathcal{N}$ for a TRP sweep in Section 3.3. Note that for a static Hamiltonian, this requirement is true for all values of $\mathcal{N}$. Since $H(t) \approx H(t_i)$ in the i^{th} subinterval (t_{i-1}, t_i), we can apply the symmetrization procedure of Section 3.1 to this subinterval. The result is the $\mathcal{G}$-invariant effective propagator

$$\tilde{U}(t_i, t_{i-1}) = \exp\left[-(i/\hbar)\Delta t_{\mathcal{N}} \tilde{H}(t_i)\right], \tag{14}$$

where

$$\tilde{H}(t_i) = \frac{1}{|\mathcal{G}|}\sum_{i=1}^{|\mathcal{G}|} \rho_i^\dagger H(t_i) \rho_i \tag{15}$$

is the $\mathcal{G}$-invariant effective Hamiltonian for (t_{i-1}, t_i). Having the effective propagator for each subinterval, the effective group-symmetrized propagator $\tilde{U}$ for the entire time-interval $(0, t)$ is simply the time-ordered product of the $\tilde{U}(t_i, t_{i-1})$:

$$\tilde{U} = T\left[\exp\left(-i/\hbar \int_0^t d\tau \tilde{H}(\tau)\right)\right], \tag{16}$$

where T indicates a time-ordered exponential, and

$$\tilde{H}(t) = \frac{1}{|\mathcal{G}|}\sum_{i=1}^{|\mathcal{G}|} \rho_i^\dagger H(t) \rho_i. \tag{17}$$

As in Section 3.1, we assume the group-symmetrizing pulses ρ_i can be applied in a time that is much less than $\Delta t_{\mathcal{N}}/|\mathcal{G}|$.

3.3 TRP

We now describe how group-symmetrized evolution can be incorporated into a TRP sweep. For our two-qubit simulations, the target gate is the modified controlled-phase gate

$$V_{cp} = \left(\frac{1}{2}\right)\left[\left(I^1 + \sigma_z^1\right) I^2 - \left(I^1 - \sigma_z^1\right)\sigma_z^2\right] \tag{18}$$

which is invariant under the group $\mathcal{G} = \{I^1 I^2, \sigma_z^1 I^2, I^1\sigma_z^2, \sigma_z^1\sigma_z^2\}$. Thus $|\mathcal{G}| = 4$, and we set $\rho_1 = I^1 I^2, \ldots, \rho_4 = \sigma_z^1\sigma_z^2$. Switching over to dimensionless time, we partition the sweep time-interval $(-\tau_0/2, \tau_0/2)$ into $\mathcal{N}$ subintervals of duration $\Delta t_{\mathcal{N}} = \tau_0/\mathcal{N}$. We want $\mathcal{N}$ to be sufficiently large that the two-qubit Hamiltonian $H_2(\tau)$ is effectively constant within each subinterval. Since the interference effects arise from the twisting of the control field, we estimate the size of $\mathcal{N}$ by requiring that the angle $\Delta\phi$ swept through by the control field in a time $\Delta t_{\mathcal{N}}$ is small compared to the final twist angle $\phi_f = \phi(\tau_0/2)$. Specifically, if we require that $\Delta\phi/\phi_f < 5 \times 10^{-3}$, and noting that $\Delta\phi(\tau) \approx \dot{\phi}(\tau)\Delta t_{\mathcal{N}}$ is largest at $\tau = \tau_0$, it follows that

$$\begin{aligned} \Delta t_{\mathcal{N}} &= \Delta\phi/\dot{\phi} \\ &< 0.005[\phi_f/\dot{\phi}(\tau_0/2)] \\ &< 7.5 \times 10^{-2}. \end{aligned}$$

Recalling that $\Delta t_{\mathcal{N}} = \tau_0/\mathcal{N}$, and noting that $\tau_0 = 120$ for the two-qubit simulations (see Section 4.2), one finds that

$$\mathcal{N} > 1600.$$

We shall see in Section 4.2 that $\mathcal{N} = 2500$ in the two-qubit simulations which produces an even smaller $\Delta\phi/\phi_f$, and so enhances the approximation of a constant $H_2(\tau)$ in each subinterval.

The two-qubit numerical simulations for group-symmetrized TRP partition the sweep interval $(-\tau_0/2, \tau_0/2)$ into $\mathcal{N}$ subintervals as just described. Each subinterval (t_{i-1}, t_i) is further partitioned into $|\mathcal{G}| = 4$ sub-subintervals by introducing intermediate times $t_{i,j} \equiv t_{i-1} + j(\Delta t_{\mathcal{N}}/4)$, with $j = 1, \ldots, 4$. The numerical integration over the i^{th} subinterval begins by driving the quantum state using a TRP sweep from $t_{i-1} \to t_{i,1}$, at which time the group-symmetrizing pulse $\rho_2\rho_1^\dagger$ is applied. The integration then resumes with TRP evolving the

state from $t_{i,1} \rightarrow t_{i,2}$, followed by application of $\rho_3\rho_2^\dagger$ at time $t_{i,2}$. This alternation of TRP-driven evolution and group-symmetrizing pulses continues until the final time t_i is reached. The numerical integration begins at $-\tau_0/2$ and continues across the subintervals until the final time $\tau_0/2$ is reached. Note that the time required to apply the group-symmetrizing pulses is assumed to be much shorter than $\Delta t_{\mathcal{N}}/4$. These pulses are applied in the simulation as matrix operations on the state. This is consistent with our bang-bang assumption, although it precludes a study of the effects of pulse imperfections on gate performance. This limitation will be removed in future work. Completion of the numerical integration yields the $\mathcal{G}$-symmetrized TRP propagator $\tilde{U}$ corresponding to a particular choice of the sweep parameters $(\lambda, \eta_4, \tau_0)$ and system parameters $(c_4, d_1, \ldots, d_4)$. $\tilde{U}$ then serves as U_a in the simulated annealing optimization which returns optimized values for the sweep and system parameters, as well as the group-symmetrized gate $\tilde{U}_a$ that best approximates the modified controlled-phase gate V_{cp}. To reduce the size of the search space, only (η_4, c_4, d_1, d_4) are optimized; $(\tau_0, \lambda, d_2, d_3)$ are assigned values. The results of this simulation/symmetrization/optimization procedure appear in Section 4.2. We shall see below that $\mathcal{G}$-symmetrized TRP yields an approximation to V_{cp} with $P_e < 10^{-4}$.

4 Simulation Results

Here we present our simulation results for the TRP-driven approximations to the gates in the universal set $\mathcal{G}_U$. The one-qubit gates are discussed in Section 4.1, while the two-qubit modified controlled-phase gate appears in Section 4.2.

4.1 One-qubit Gates

Operator expressions for the one-qubit target gates in $\mathcal{G}_U$ are:

$$\begin{aligned}
\textit{Hadamard}: &\quad U_h = (1/\sqrt{2})\,(\,\sigma_z + \sigma_x\,)\,; \\
\textit{NOT}: &\quad U_{not} = \sigma_x; \\
\textit{Modified } \pi/8: &\quad V_{\pi/8} = \cos(\pi/8)\;\sigma_x - \sin(\pi/8)\;\sigma_y; \\
\textit{Modified phase}: &\quad V_p = (1/\sqrt{2})\,(\,\sigma_x - \sigma_y\,)\,.
\end{aligned}$$

A study of the TRP-implementation of these gates was first reported in Ref. [12]. The essential results are included here for the reader's convenience, though space limitations do not allow inclusion of the unitary operator U_a associated with each gate. The interested reader can find them displayed in Ref. [12]. The connection between the TRP experimental and theoretical parameters is given in Refs. [10] and [12] for superconducting and NMR qubits, respectively.

Table 1 presents the values for the sweep parameters λ and η_4 that produced our best

Table 1. Simulation results for the one-qubit gates in $\mathcal{G}_U$. The error probability for each gate satisfies $P_e \leq Tr\,P$.

Gate	λ	η_4	$Tr\,P$	$\mathcal{F}$
Hadamard	5.8511	2.9280×10^{-4}	8.82×10^{-6}	0.9999 98
NOT	7.3205	2.9277×10^{-4}	1.10×10^{-5}	0.9999 97
Modified $\pi/8$	6.0150	8.1464×10^{-4}	3.03×10^{-5}	0.9999 92
Modified phase	5.9750	3.8060×10^{-4}	8.20×10^{-5}	0.9999 80

results for $Tr\,P$ for each of the one-qubit gates in $\mathcal{G}_U$. In all one-qubit simulations, the dimensionless inversion time was $\tau_0 = 80.000$. Since $P_e \leq Tr\,P$, we see that $P_e < 10^{-4}$ for all

one-qubit gates in $\mathcal{G}_U$. Table 1 also gives the fidelity $\mathcal{F}$ for each gate which is obtained from $Tr\,P$ via Eq. (11). We will discuss the robustness of these gates in Section 5.

4.2 Modified Controlled-phase Gate

We complete the universal set $\mathcal{G}_U$ by presenting our simulation results for the $\mathcal{G}$-symmetrized TRP implementation of the modified controlled-phase gate V_{cp}. In the two-qubit computational basis (eigenstates of $\sigma_z^1\sigma_z^2$),

$$V_{cp} = \begin{pmatrix} 1 & 0 & 0 & 0 \\ 0 & 1 & 0 & 0 \\ 0 & 0 & -1 & 0 \\ 0 & 0 & 0 & 1 \end{pmatrix} . \tag{19}$$

TRP implementation of V_{cp} *without* symmetrized evolution was reported in Ref. [10]. The results presented there are superceded by the $\mathcal{G}$-symmetrized TRP results presented here.

For purposes of later discussion, note that the parameters appearing in $\mathcal{H}_2(\tau)$ (see Eq. (6)) fall into two sets. The first set consists of the TRP sweep parameters $(\lambda, \eta_4, \tau_0)$, while the second set $(c_4, d_1, \ldots, d_4)$ consists of system parameters for degeneracy-breaking, detuning, and coupling. We partitioned the TRP sweep into $\mathcal{N} = 2500$ pulses sequences, with each sequence based on the four element symmetry group $\mathcal{G}$ for V_{cp} introduced in Section 3.3. The optimized parameter values $\lambda = 5.04$, $\eta_4 = 3.0 \times 10^{-4}$, $\tau_0 = 120.00$, $c_4 = 2.173$, $d_1 = 99.3$, $d_2 = 0.0$, $d_3 = -0.41$, and $d_4 = 0.8347$ produced the following two-qubit gate U_a:

$$Re\ (U_a) = \begin{pmatrix} 0.9999\,98 & -0.0000\,03 & -0.0000\,15 & -0.0000\,14 \\ 0.0000\,03 & 0.9999\,97 & 0.0000\,36 & 0.0002\,61 \\ -0.0000\,15 & 0.0000\,34 & -0.9999\,80 & -0.0038\,18 \\ -0.0000\,14 & -0.0002\,57 & -0.0038\,38 & 0.9999\,81 \end{pmatrix} ; \tag{20}$$

$$Im\ (U_a) = \begin{pmatrix} -0.0021\,51 & 0.0000\,03 & -0.0000\,10 & -0.0000\,73 \\ -0.0000\,03 & -0.0021\,80 & 0.0001\,40 & -0.0003\,25 \\ 0.0000\,10 & -0.0011\,40 & 0.0017\,02 & 0.0045\,34 \\ -0.0000\,73 & -0.0003\,28 & -0.0045\,21 & -0.0017\,78 \end{pmatrix} . \tag{21}$$

From U_a and $U_t = V_{cp}$, we find: (i) $Tr\,P = 8.87 \times 10^{-5}$; (ii) gate fidelity $\mathcal{F}_{cp} = 0.9999\,89$; and (iii) $P_e \leq 8.87 \times 10^{-5}$. We see that by adding symmetrized evolution to a TRP sweep we obtain an approximation to V_{cp} with $P_e < 10^{-4}$.

We see that it has been possible to use TRP sweeps to produce a high-fidelity universal set of quantum gates $\mathcal{G}_U$, with each gate error probability falling below the rough-and-ready estimate for the accuracy threshold for fault-tolerant quantum computing: $P_e < 10^{-4}$.

5 Discussion

We have presented simulation results which suggest that TRP sweeps should be capable of implementing the universal quantum gate set $\mathcal{G}_U$ non-adiabatically and with gate error probabilities satisfying $P_e < 10^{-4}$. It is worth noting that all gates in $\mathcal{G}_U$ are driven by a *single* type of control field (TRP), and that the gate error probability for all gates in $\mathcal{G}_U$ falls below the rough-and-ready estimate of the accuracy threshold $P_a \sim 10^{-4}$. These results suggest that TRP sweeps show promise for use in a fault-tolerant scheme of quantum computing.

To achieve this high level of performance in our current formulation of TRP, some of the TRP parameters must be controlled to high precision. For the one-qubit gates [12], the critical parameter is η_4 which must be controlled to five significant figures to achieve best gate performance. For the modified controlled-phase gate V_{cp}, the critical parameters are *not* the TRP sweep parameters. Instead, for V_{cp} *without* symmetrized evolution [10], the critical parameters are c_4, d_1, and d_4 which also require five significant figure precision. However, *when group-symmetrized evolution is added*, not only is TRP able to make an approximate V_{cp} with $P_e < 10^{-4}$, but gate robustness is also *improved*. Specifically, d_1 ceases to be a critical parameter, and c_4 and d_4 now only need to be controllable to four significant figures. Table 2 shows how $Tr\,P$ varies when either c_4 or d_4 is varied in the fourth significant figure, with all

Table 2. Sensitivity of $Tr\,P$ to small variation of c_4 and d_4 for the two-qubit gate V_{cp}. All other parameter values are as given in the text.

c_4	$Tr\,P$	d_4	$Tr\,P$
2.172	6.79×10^{-3}	0.8346	1.52×10^{-3}
2.173	8.87×10^{-5}	0.8347	8.87×10^{-5}
2.174	7.73×10^{-3}	0.8348	1.52×10^{-3}

other parameters held fixed. Thus, adding group-symmetrized evolution improves both the accuracy and robustness of the TRP approximation to V_{cp}. Note that four significant figure precision corresponds to 14-bit precision which can be realized with present-day arbitrary waveform generators (AWG) [20]. On the other hand, the current precision requirements for all one-qubit gates in $\mathcal{G}_U$ lie beyond the reach of existing commercially available AWGs. Unfortunately, group-symmetrized evolution cannot be used to improve the robustness of the one-qubit TRP gates. It is possible to show that if $U_t = \mathbf{a} \cdot \boldsymbol{\sigma}$, the only one-qubit unitary operators that commute with U_t are the identity and a multiple of U_t. Thus the only symmetry group available that does not include U_t is the trivial group whose sole member is the identity. Some other means must be found to improve the robustness of the TRP approximations to the one-qubit gates in $\mathcal{G}_U$. Two approaches are currently under study based on: (i) the Hessian of our cost function $Tr\,P$; and (ii) quantum optimal control theory.

In previous work [21] we have studied a number of forms of polynomial, as well as periodic, twist. To date we have found that quartic twist provides best all-around performance when it comes to making the gates in $\mathcal{G}_U$. Although we do not at present have arguments that explain why this is so, ongoing work based on quantum optimal control provides a framework with which this question can be studied. This represents an important direction for future work.

Finally, Refs. [10]– [12] have shown how TRP sweeps can be applied to NMR, atomic, and superconducting qubits. We note that TRP-generated quantum gates should also be applicable to spin-based qubits in quantum dots as such qubits also Zeeman-couple to a magnetic field.

Acknowledgements

We thank: (i) F. Nori, RIKEN, and CREST for making our visit to RIKEN possible;(ii) RIKEN for access to the RIKEN Super Combined Cluster on which the simulations incorporating group-symmetrized evolution were done; and (iii) T. Howell III for continued support.

References

1. D. Aharanov and M. Ben-Or, *Fault-tolerant computation with constant error*, in Proceedings of the Twenty-Ninth ACM Symposium on the Theory of Computing, 176 (1997).
2. A. Y. Kitaev, *Quantum computation algorithms and error correction*, Russ. Math. Surv. **52**, 1191 (1997).
3. A. Y. Kitaev, *Quantum error correction with imperfect gates*, in Quantum Communication, Computing, and Measurement (Plenum Press, New York, 1997), pp. 181–188.
4. D. Gottesman, *Stabilizer codes and quantum error correction*, Ph. D. thesis, California Institute of Technology, Pasadena, CA (1997).
5. E. Knill, R. Laflamme, and W. H. Zurek, *Resilient quantum computation*, Science **279**, 342 (1998).
6. E. Knill, R. Laflamme, and W. H. Zurek, *Resilient quantum computation: error models and thresholds*, Proc. R. Soc. Lond. A **454**, 365 (1998).
7. J. Preskill, *Reliable quantum computers*, Proc. R. Soc. Lond. A **454**, 385 (1998).
8. F. Gaitan, *Quantum error correction and fault-tolerant quantum computing* (CRC Press, Boca Raton, FL 2008).
9. J. W. Zwanziger, S. P. Rucker, and G. C. Chingas, *Measuring the geometric component of the transition probability in a two-level system*, Phys. Rev. A **43**, 3232 (1991).
10. R. Li, M. Hoover, and F. Gaitan, *High-fidelity universal set of quantum gates using non-adiabatic rapid passage*, Quantum Info. Comp. **9** 290 (2009).
11. F. Gaitan, *Temporal interferometry: a mechanism for controlling qubit transitions during twisted rapid passage with a possible application to quantum computing*, Phys. Rev. A **68** 052314 (2003).
12. R. Li, M. Hoover, and F. Gaitan, *High-fidelity single-qubit gates using non-adiabatic rapid passage*, Quantum Info. Comp. **7** 594 (2007).
13. J. W. Zwanziger, U. Werner-Zwanziger, and F. Gaitan, *Non-adiabatic rapid passage*, Chem. Phys. Lett. **375** 429 (2003).
14. P. Zanardi, *Symmetrizing evolutions*, Phys. Lett. A **258** 77 (1999).
15. A. Abragam, *Principles of nuclear magnetism* (Oxford University Press, New York 1961).
16. F. Gaitan, *Berry's phase in the presence of a non-adiabatic environment with an application to magnetic resonance*, J. Mag. Reson. **139** 152(1999).
17. R. P. Feynman and A. R. Hibbs, *Quantum mechanics and path integrals*, (McGraw-Hill, New York, 1965).
18. W.H. Press et al., *Numerical Recipes* (Cambridge University Press, New York 1992).
19. L. Viola and S. Lloyd, *Dynamic suppression of decoherence in two-state quantum systems*, Phys. Rev. A **58**, 2733 (1998).
20. For example, the Tektronix AWG5000B arbitrary waveform generator provides 14-bit vertical resolution.
21. R. Li and F. Gaitan, *Controlling qubit transitions through quantum interference during non-adiabatic rapid passage*, Optics and Spectroscopy **99**, 257 (2005).